Bull. Mater. Sci., Vol. 31, No. 4, August 2008, pp. 687–691. © Indian Academy of Sciences.

Surface hardness behaviour of Ti–Al–Mo alloys

RAJA RAM PRASAD, SHANKAR AZAD, A K SINGH† and R K MANDAL*

Department of Metallurgical Engineering, Banaras Hindu University, Varanasi 221 005, India
†Defence Metallurgical Research Laboratory, Hyderabad 500 058, India

MS received 26 September 2007; revised 4 March 2008

Abstract. The microhardness characteristics of various micro-constituents formed in the Ti–Al–Mo alloys have been investigated. Four alloys having compositions, Ti–40Al–2Mo, Ti–42Al–2Mo, Ti–40Al–6Mo and Ti–42Al–6Mo, have been chosen for this purpose. All of these were heat treated at 1300°C and 1400°C for 1 h and water quenched. All the specimens after above heat treatments have displayed load independent Vickers hardness values (VHN) around 300 g of applied load. The average surface hardness characteristic of the alloys is largely found to be dictated by the phases that are present. The microstructural specific VHN values vary between 600 and 750. The indentation behaviour, however, is governed by the morphologies and length scales of microstructures. The most remarkable finding of the present study pertains to the formation of shear bands around the periphery of the indenter for a finer basket weave microstructure in the Ti–40Al–2Mo. The cluster of finely located slip steps was clearly seen. Such a report is lacking in literature in this class of alloys.

Keywords. Ti–Al–Mo alloys; microhardness; slip steps.

1. Introduction

Ti-aluminides containing α_2 and γ phases with lamellar morphology are expected to possess hardness that is higher than the β and γ phases (Li and Loretto 1994). Room temperature ductility is the most important impediment in the way of their applicability as high temperature structural material. Alloys with two phases (α_2 and γ) have demonstrated an inverse correlation between their tensile properties and resistance to fracture (Saari *et al* 2005). It has, therefore, been essential to suggest morphologies of these alloys that can yield optimum blend of properties. The inhomogeneity in microstructure while processing these materials has made analysis further difficult in delineating any issues pertaining to above. The intensified research (Banerjee *et al* 2005) on Ti–Al–Nb system to attain this goal, led to the discovery of ordered orthorhombic O phase. This has given rise to improvement of properties. Following this, other ternary additions (Mo, V, W, Cr, Ta etc) have been made (Djanarthany *et al* 1992; Kainuma *et al* 2000). Mo is the strongest β stabilizer. Ordered B2 phase is expected to improve the room temperature deformation behaviour as well as its creep strength (Germann *et al* 2005).

The brittle characteristics of these alloys have made the preparation of samples for the mechanical testing a very difficult enterprise. Keeping this in view, the present work has been undertaken. It has been argued in literature that indentation hardness measurement can permit us to infer about the mechanical behaviour of the material (Zhang *et al* 2003). Li and Loretto (1994) have carried out such studies for Ti–44Al–2Mo on their Hipped samples. In this presentation, load dependent surface and microhardness characteristics of four alloys after heat treatment will be reported. The primary aim of this work is to understand the influence of morphologies, length scales and compositions of the alloys on the hardness characteristics as well as on the nature of indentation. Later, recent investigations on indentation characteristics of bulk metallic glasses and nanocrystalline materials have received wider attention as shear band that formed around the indentation periphery contain information about the nature of load displacement curve of the material (Zhang *et al* 2003; Ramamurthy *et al* 2005; Tang *et al* 2005). Such a viewpoint is lacking in literature containing studies on the Ti-aluminides. It has, therefore, been thought appropriate to lay proper emphasis on the analysis of the nature of indentation. For this, the results of a series of microstructural features under micro-indentation will be reported for the same alloy compositions. The formation of shear band in one of the alloys will be discussed in the light of latest trend in indentation studies (Viadyanathan *et al* 2001; Zhang *et al* 2005).

2. Experimental

Alloys of four different compositions were prepared using vacuum arc melting furnace in the form of pancake. Table 1 gives the alloy compositions and the condition of heat

*Author for correspondence (rkmandal21@yahoo.com)

Table 1. Nominal compositions of different alloys and their designation in various heat-treated conditions.

Sl. no.	Nominal composition	Alloy designation		
		As cast	1300°C/1 h/WQ	1400°C/1 h/WQ
1	Ti–40Al–2Mo	Sample 1	HT11	HT21
2	Ti–42Al–2Mo	Sample 2	HT12	HT22
3	Ti–40Al–6Mo	Sample 3	HT13	HT23
4	Ti–42Al–6Mo	Sample 4	HT14	HT24

Table 2. Summary of X-ray diffraction results. Major phases present in the alloys are indicated in bold letters (Azad *et al* 2006).

Sl. no.	Nominal composition	Phases present		
		As cast	1300°C/1 h/WQ	1400°C/1 h/WQ
1	Ti–40Al–2Mo	γ, β, α_2	γ, β, α_2	γ, β, α_2
2	Ti–42Al–2Mo	γ, β, α_2	γ, $\boldsymbol{\beta}$, α_2	γ, $\boldsymbol{\beta}$, α_2
3	Ti–40Al–6Mo	γ, $\boldsymbol{\beta}$	$\boldsymbol{\beta}$, α_2	γ, $\boldsymbol{\beta}$, α_2
4	Ti–42Al–6Mo	γ, $\boldsymbol{\beta}$	$\boldsymbol{\beta}$	γ, β, α_2

treatment given to them. To understand the effect of Mo addition, alloys were given two different solution treatments in the single β phase field based on the information available with binary phase diagram of Ti–Al and Ti–Al–Mo systems (Murray 1988; Kattnar *et al* 1992; Budberg and Schmid-Fetzer 1993). The first solutionizing treatment was given at 1300°C and the other at 1400°C for 1 h. Samples were coated with Delta glaze to prevent oxygen pick up during heat treatment. After solutionizing, specimens were quenched in water to retain the β phase. The nomenclature followed for different alloys in the present study is given in table 1. The X-ray diffraction (XRD) experiments were carried out by Philips X-ray diffractometer for well-polished bulk specimens of as cast samples and on Rigaku DMAX-III (both with copper target) for powders of heat-treated samples. Microhardness measurements of all the heat treated samples were performed with the help of SHIMADZU HMV-2T microhardness tester at different loads i.e. 50, 100, 200, 300, and 500 g. The hardness measurements were carried out on many of the characteristics microstructural features of the heat-treated alloys. These were done to understand the role of morphology and length scale of various microconstituents on the indentation behaviour.

3. Results

Microstructural and X-ray diffraction results of these samples have been published earlier (Azad *et al* 2006). Table 2 gives summary of the results arrived at based on X-ray diffraction results. The load dependent hardness behaviour of the heat-treated specimen is shown in figure 1(a) for solution treated at 1300°C for 1 h followed by quenching. It may be noted that load independent hardness for HT11 and HT13 appears at 300 g of applied load whereas for HT12 and HT14, load independent hardness is achieved at 100 g load. Further, the HT22 samples have shown lowest hardness values. Figure 1(b) displays the load dependent behaviour of hardness of all the four alloys solutionized at 1400°C for 1 h followed by water quenching. Nearly similar surface hardness behaviours have been observed with respect to load for HT21, HT23 and HT24. However, for HT22, the hardness value has been lowered down significantly. The load independent hardness has appeared beyond 300 g load. Microhardness characteristics of various microstructural features studied in the present investigation are reported in table 3. We note that load independent hardness occurs beyond 300 g of load excepting that of gray plate morphology of HT22. Figure 2(a) displays the indentation mark at various loads in a single α_2 plate for HT11 specimen. Figures 2(b) and (c) display unusual indentation characteristics of the HT11 specimen having basket weave morphology.

4. Discussion

Having presented the results of surface and microhardness behaviour of the alloys, attempt will now be made to understand the unique feature of indentation shown in figures 2(b) and (c). Further, owing to non-availability of similar studies it will not be possible to compare the results with those of the others. Li and Loreto (1994) have reported microhardness of various phases in this system. The specimens in their case were hipped. The measured Vickers hardness values were 444 VHN for B2 phase, 297 VHN for the γ phase and 552 VHN for ($\alpha_2 + \gamma$) phase,

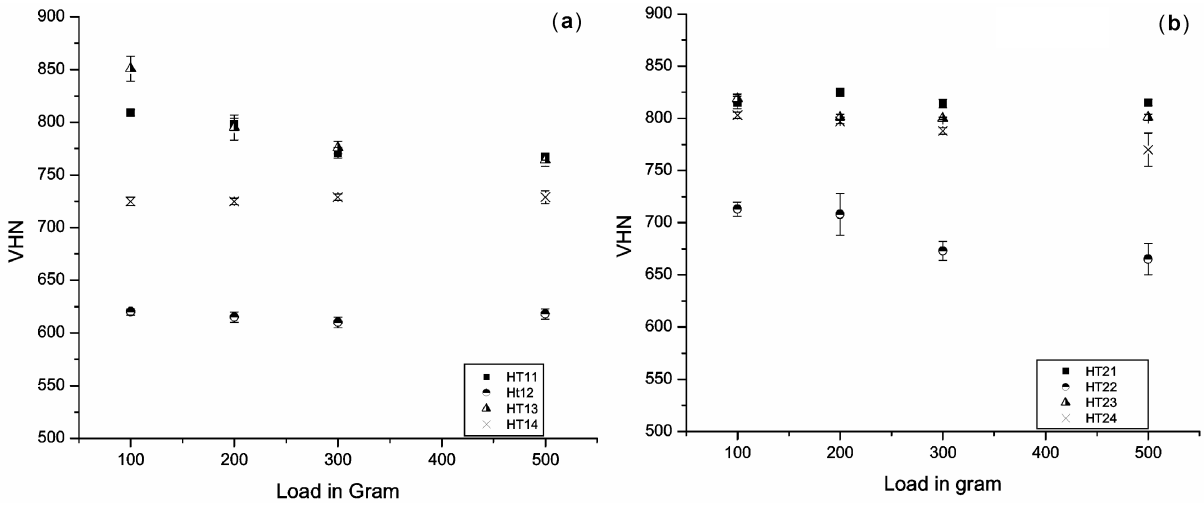

Figure 1. VHN vs load graph: (**a**) variation of hardness with respect to load for specimen in HT1 condition and (**b**) in HT2 condition.

Table 3. Microhardness for various morphologies in the heat-treated alloys.

		VHN with standard deviation at indentation load (g)			
Sample	Morphology (phase(s))	100	200	300	500
HT11	Fine basket weave ($\alpha_2 + \gamma$)	809 (±6)	798 (±6)	771 (±5)	767 (±3)
HT12	Acicular (AC) (α_2)	620 (±3)	615 (±5)	610 (±5)	618 (±5)
	Coarse lamellae (CL) (α_2)	646 (±6)	628 (±7)	618 (±7)	622 (±3)
	Fine lamellae (FL) (α_2)	740 (±15)	760 (±4)	752 (±3)	709 (±7)
	Basket weave (BW) ($\alpha_2 + \gamma$)	734 (±12)	755 (±4)	748 (±4)	745 (±4)
HT13	Single phase (β)	851 (±12)	795 (±12)	776 (±6)	764 (±6)
HT14	Single phase (β)	725 (±4)	725 (±3)	729 (±3)	729 (±3)
HT21	Lamellae ($\alpha_2 + \gamma$)	815 (±6)	825 (±4)	814 (±4)	815 (±3)
HT22	Lamellae (L) ($\alpha_2 + \gamma$)	713 (±7)	708 (±20)	673 (±9)	665 (±15)
	Gray plate (GP) (γ)	678 (±13)	650 (±10)	637 (±2)	723 (±9)
HT23	Single phase (β)	819 (±4)	801 (±3)	800 (±1)	801 (±3)
HT24	Single phase (β)	803 (±3)	797 (±2)	788 (±3)	770 (±16)

which indicates that the hardness of the B2 phase lies between α_2 and γ. In the present investigation, the load independent surface hardness values for HT11 and HT13 have been found to be around 775 VHN for both of them although, the microstructural and structural ingredients are different. For example, the indentation characteristics of figure 2 clearly demonstrate the presence of basket weave morphology at a very finer scale containing α_2 and γ as major phases. In contrast to this, the hardness values observed from figure 1 for HT13 correspond to nearly single-phase β with α_2 as a minor constituent. It is important to note here that around the indentation the flow of material can be noted in figure 2 that was absent for HT13 specimen. The formation of slip steps (see the arrows marked in figures 2b and c) with irregular bands around the indentation periphery is usually described in the current literature as shear bands. The formation of shear bands at low load indicates initiation of plastic deformation along with the elastic component (Zhang *et al* 2005). Such a behaviour in the present investigation was observed only for HT11 alloy having fine basket weave microstructure. The hardness values in conjunction with the shear band formation clearly bring out the importance of structure, morphology and length scale of microstructures. There have been intense studies in the area of shear band formation in the ultra fine grain microstructures with the help of strain gradient plasticity (Zhang *et al* 2003). This novel finding in the class of Ti–Al–Mo alloys containing α_2 and γ phases with basketweave morphology will definitely offer the researchers good material for further studies. It has been reported in the literature that below the surface of the material, a large strain gradient is expected (Viadyanathan *et al* 2001; Zhang *et al* 2003, 2005; Ramamurthy *et al* 2005; Tang *et al* 2005). Verification of strain gradient plasticity through geometrically necessary dislocation or statistical introduction of dislocation during

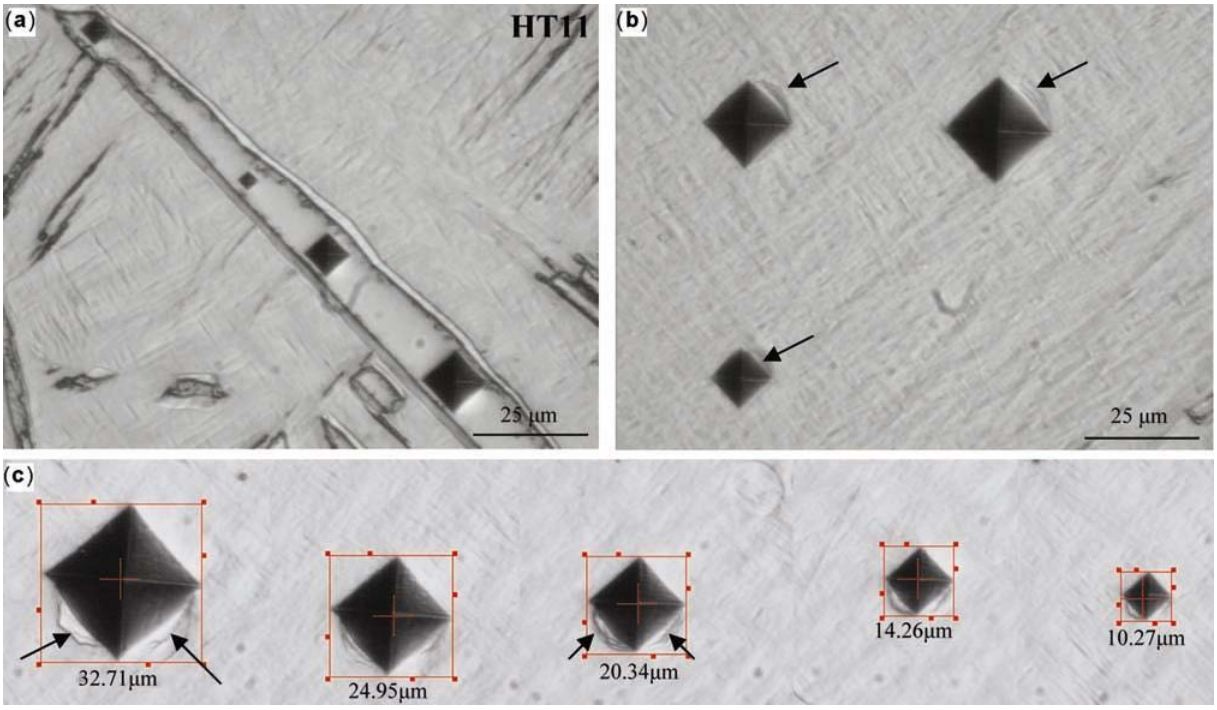

Figure 2. (**a**) Indentation in a coarse α_2 plate at different loads, (**b**) nature of indentation at various loads for fine basket weave morphology displaying fine slip steps (see the arrows) around the indentation periphery and (**c**) presence of finely spaced slip-steps (marked by arrows) in the basket weave morphology at different loads. Five indentation impressions from various regions of the sample are superimposed.

indentation is a difficult exercise to attain in absence of availability of large specimen for bend and torsion test for bulk metallic glasses as well as for nano-structured materials (Viadyanathan *et al* 2001). It is believed that by adopting appropriate heat treatment procedure for alloys containing intermetallic phases such studies will be facilitated. It is hoped that investigations akin to the present one, on alloys having micro constituents distributed over a length scale of ~ 100 nm will be revisited from the present perspective to throw light on the nature of shear band formation.

5. Conclusions

The microhardness characteristics of various microconstituents formed in the Ti–Al–Mo alloys have been reported in this paper. In all the heat-treated alloys, the Vicker's microhardness values have displayed load independent VHN around 300 g of load. The average surface hardness characteristics of the alloys are largely found to be dictated by the phases that are present. The microstructural specific VHN values vary between 600 and 750. The indentation behaviour, however, is governed by the morphologies and length scales of microstructures. The most remarkable finding conforming to the above assertion is corroborated by the formation of shear bands around the periphery of the indenter for a finer basket weave microstructure for the alloy Ti–40Al–2Mo (1300°C/1 h/WQ). The cluster of finely located slip steps is clearly seen. Such a finding is lacking in literature in this class of alloys. It is believed that this report will facilitate further studies in this area and it will be possible to study the mechanism of shear band formation of materials at submicroscopic length scales.

Acknowledgements

Authors thank Prof. S Lele, Rector, Banaras Hindu University, Varanasi and Director, Defence Metallurgical Research Laboratory, Hyderabad, for encouragement.

References

Azad Shankar, Mandal R K and Singh A K 2006 *Mater. Sci. & Eng.* **A429** 219

Banerjee D, Gogia A K, Nandi T K and Joshi V A 2005 *Acta Mater.* **36** 871

Budberg P and Schmid-Fetzer R 1993 in *Ternary alloys: A comprehensive compendium of evaluated constitutional data and phase diagrams* (eds) G Petzow and G Effenberg (Weinheim, Germany: VCH) **37** pp 229–238

Djanarthany S, Servant C and Penelle R 1992 *Mater. Sci. & Engg.* **A152** 48

Germann L, Banerjee D, Guedou J Y and Strudel J L 2005 *Intermetallics* **13** 920

Kainuma R, Fujita Y, Mitsui H, Ohnuma I and Ishida K 2000 *Intermetallics* **8** 855

Kattnar U R, Lin J C and Chang Y A 1992 *Met. Trans.* **A23** 2081

Li Y G and Loretto M H 1994 *Acta Metal. Mater.* **42** 2913

Murray Joanne L 1988 *Metall. Trans.* **A19** 243

Ramamurthy U, Jana S, Kawamura Y and Chattopadhyay K 2005 *Acta Mater.* **53** 705

Saari H, Beddoes J, Seo D Y and Zhao L 2005 *Intermetallics* **13** 937

Tang Chunguag, Li Yi and Zeng Kai Yang 2005 *Mater. Lett.* **59** 3325

Viadyanathan R, Dao M, Ravichandran G and Suresh S 2001 *Acta Mater.* **49** 781

Zhang Hongwen, Subhash Ghatu, Kecskes Laszlo J and Dowding Robert J 2003 *Scr. Mater.* **49** 447

Zhang Hongwen, Jing Xiaoning, Subhash Ghatu, Kecskes Laszlo J and Dowding Robert J 2005 *Acta Mater.* **53** 3849